Deuterium retention in MeV ion-irradiated beryllium

Anže Založnik[1], Russell P. Doerner[1], Thomas Schwarz-Selinger[2], Mitsutaka Miyamoto[3], Sebastijan Brezinsek[4]

[1]Center for Energy Research, University of California at San Diego, 9500 Gilman Dr, La Jolla, CA 92093, USA

[2]Max-Planck-Institut für Plasmaphysik, Boltzmannstrasse 2, D-85748 Garching, Germany

[3]Department of Material Science, Shimane University, 1060 Nishikawatsu, Matsue, 690-8504, Japan

[4]Forschungszentrum Jülich GmbH, Institut für Energie und Klimaforschung - Plasmaphysik, 52425 Jülich, Germany

Abstract

Beryllium, as the material of choice for the ITER first wall, will be subject to high energy neutrons during the operation of the fusion device. Such irradiation will create displacement damage in the crystal lattice, which is known to influence hydrogen isotope retention, e.g. in iron and tungsten. In our study, we irradiated beryllium samples with high-energy oxygen ions up to various dpa levels (0.01 dpa, 0.1 dpa, and 1 dpa) and subsequently exposed the samples to deuterium plasma at 370 K and 573 K. The amount of retained deuterium was measured by thermal desorption spectroscopy and nuclear reaction analysis and was found to decrease by about 18% in the samples damaged up to 0.1 dpa compared to the undamaged ones. Further damaging up to 1 dpa did not show any additional effects on deuterium retention. Transmission electron microscopy was used to check for the existence of bubbles after plasma exposure.

1 Introduction

During the operation of a fusion device, the inner wall and other plasma-facing components will be subject to high particle and heat fluxes. High-energy ions and especially neutrons will create defects in the material, such as vacancies, interstitials, dislocations, and clusters of coalesced defects. In addition to displacement damage, neutrons will also cause transmutations in the material. All this will change the properties of the material and limit its lifetime.

In ITER, tungsten (W) and beryllium (Be) will be used for the divertor and the first wall, respectively. The damage level for Be at the end of the machine's lifetime is predicted to be less than 3 dpa. In the case of W, the effect of damaging on the properties of the material has been extensively studied experimentally and theoretically. It has been found that damaging degrades the favorable properties of W, e.g. reduces thermal conductivity [1, 2] and increases hydrogen isotope retention [2–5]. In W, defects act as strong binding sites for hydrogen isotopes leading to a strong increase of their retention compared to undamaged W. Moreover, since the thermal conductivity decreases, the heating of damaged W plasma-facing components is severely enhanced. On the other hand, studies of the effects of damaging on Be properties are much scarcer and focus mostly on transmutation and the effects on the microstructure of neutron-irradiated material, e.g. [6–8]. To our knowledge, there have been no studies on hydrogen isotope retention in damaged Be.

Due to the difficulties with neutron sources and sample activation, neutron damaging is often mimicked by damaging with high-energy heavy ions. One of the differences between the two is that the range of ions in the material is much shorter compared to neutrons, however, it is believed that both techniques create similar displacement damage in the crystal lattice of the material [9]. Therefore, heavy ions can in some cases be a good surrogate for neutron irradiation when studying displacement damage. It is not clear to what extent this is true for ion-damaged Be, therefore rather than providing a direct extrapolation to neutron irradiation, this work should serve as a basic study of the physics of defect creation, evolution, and their interaction with hydrogen isotopes.

2 Experiment

For this study identical S-65 grade hot-pressed Be samples with a diameter of 8 mm and a thickness of 2 mm were used. The samples were provided by Materion and contain a minimum of 99.2% beryllium and a maximum of 0.9% beryllium oxide. All other elements (such as Al, C, Fe...) are in trace amounts with less than 0.1%. Five samples were pre-damaged at room temperature by high-energy oxygen (O) ions up to various dpa levels (0.01, 0.1 and, 1 dpa). Oxygen was used in order to avoid an introduction of any new impurities in the samples, since it is already naturally occurring in Be. It was implanted in the "sak" beamline of the tandem accelerator at Max-Planck-Institut für Plasmaphysik (IPP) [10]. We were able to achieve a quasi-flat damage depth profile, oscillating around the nominal dpa level by about 10%, using six different ion beam energies. The energies and corresponding ion fluences needed to achieve a damage level of 1 dpa are summarized in Table 1. The total O fluence was 29.9×10^{15} O/cm^2, which results in an average of 0.12% of additional O over a 2 μm damaged layer. For lower dpa levels the fluences were accordingly scaled and additional O contamination correspondingly lower. The typical BeO content for S-65 grade Be is no more than 0.9%. The resulting damage depth profile was obtained by analyzing the "vacancy.txt" file, output by SRIM software [11]. The calculation was performed in "quick calculation" mode with displacement energy of 25 eV. The damage depth profile is shown in Fig. 1.

Table 1: Oxygen ion beam energies and corresponding fluences, used to achieve 1 dpa quasi-homogeneous damage depth profile.

energy [keV]	fluence [10^{15} O/cm^2]
400	9.6
550	4.9
725	4.5
950	3.9
1200	3.4
1500	3.6

After the damaging, each sample was mounted on a sample holder in the PISCES-B linear plasma device [12]. A Be mask and cap were used to fix the sample in position in order to avoid sputtering and the deposition of impurities on the sample. The Be mask limited the effective diameter of the area actually exposed to plasma to 6 mm. The samples were exposed

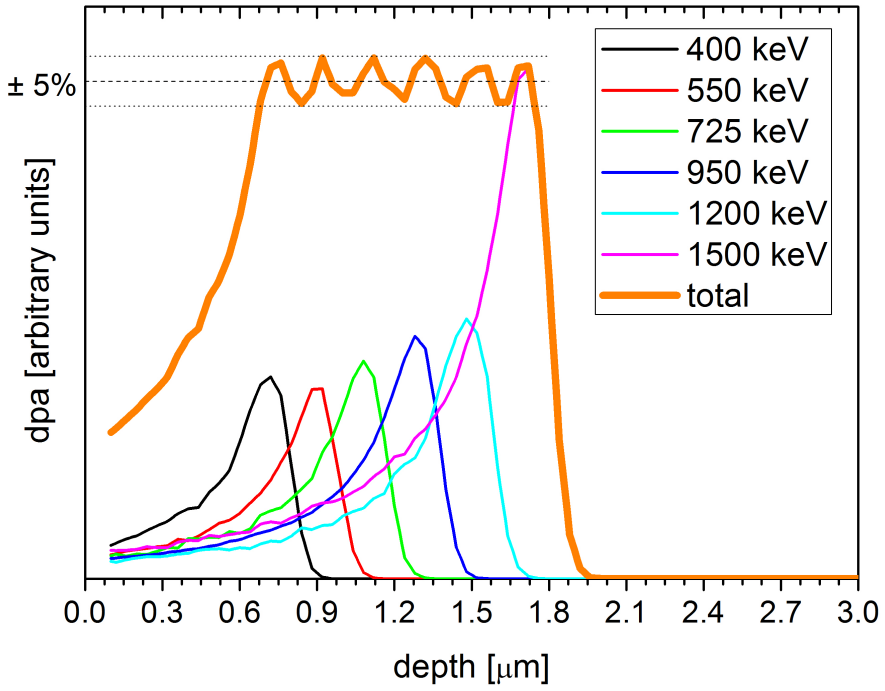

Figure 1: The damage profile after O ion irradiation with 6 different energies as calculated by SRIM software.

to deuterium (D) plasma at two different exposure temperatures, 370 K (undamaged, 0.1 dpa, and 1 dpa) and 573 K (undamaged, 0.01 dpa, 0.1 dpa, and 1 dpa), which were obtained and kept constant by controlling the flow of the cooling air within the sample manipulator. The sample temperature was measured by a thermocouple in contact with the back side of the sample. The plasma parameters were kept constant for all exposures and were measured by a reciprocating Langmuir probe approximately 1 cm in front of the sample. The electron temperature and density were ~ 5 eV and $(2-3)\times 10^{18}$ m^{-3}, respectively. The ion flux was $(1.5-2.5)\times 10^{22}$ m^{-2}s^{-1}. The floating and plasma potential were ~ -30 eV and ~ -10 eV, respectively. Samples were biased to -50 eV, resulting in the energy of the impacting ions of ~ 40 eV. All samples were exposed to a fluence of 10^{26} D/m^2.

After the exposure, nuclear reaction analysis (NRA) was performed on each sample in the same beamline at IPP where damaging was conducted before [10]. A ^3He probing ion beam was used to determine total D amounts in the samples, utilizing $D(^3He,p)^4He$ nuclear reaction. Three ion beam energies were used, 2000 keV, 800 keV, and 500 keV, resulting in an information depth of 7.8 μm, 2.8 μm, and 1.8 μm, respectively, as calculated by SRIM. The reaction protons were measured under a reaction angle of 135°, using a thick surface barrier detector with a 5 μm Ni and 13 μm Mylar foil installed in front of it to stop the backscattered ^3He ions. A curved aperture limited the solid angle to 22 msr. For increased depth resolution at the surface, alpha particles were detected under a reaction angle of 150°

with a thin partially depleted silicon detector with a 3.5 μm Maylar foil in front of it. A 274 nm thick, plasma-deposited amorphous deuterated carbon film on silicon, with a known D to C ratio, was used as a standard for calibration. Deuterium depth profiles and areal densities were obtained using the NRADC software [13].

In addition to NRA, thermal desorption spectroscopy (TDS) was also performed. Samples exposed at 370 K were put in a quartz tube, attached to a stainless steel vacuum chamber with a background pressure in a range of 10^{-7} mbar [14]. Each sample was linearly heated by an infrared heat source up to 1222 K at a rate of 0.3 K/s. Partial pressures of desorbing species, including H_2/D, *HD* and D_2, were recorded by two residual gas analyzers (RGA). A background subtraction method [15, 16] was applied to eliminate the spurious H_2 contribution to the *HD* and D_2 signals. Both RGAs were calibrated with a D_2 leak standard with a flow rate of 1.83×10^{-9} D_2/mol s and accuracy of 3%, enabling the conversion of the RGA signal to the atomic desorption flux. The sensitivity for D_2 and *HD* was assumed to be the same.

The samples with the damage level of 0 dpa, 0.1 dpa, and 1 dpa, exposed at 573 K, were cut by a focused ion beam (FIB) and the existence of bubbles in the material was investigated using a transmission electron microscope (TEM) [17]. First, lamellas of about 30 μm $\times$ 10 μm and roughly 100 nm thick were produced by FIB micro-sampling method using HITACHI-FB-2100 with 40 kV Ga ions. Then, the microstructures of the bubbles were investigated by JEOL JEM-2010 at 200 kV in underfocus conditions. After that, TDS was performed on the remains of the FIB-cut samples, this time in a different setup than the one described before, with a heating rate of 1 K/s up to 1173 K, following the D_2 release from the samples. The background pressure in the TDS system was in a range of 10^{-8} mbar. The used RGA was calibrated with a D_2 leak standard with a flow rate of 3.57×10^{-8} Pa m^3/s and accuracy of 6.16%. The area of the FIB-cut samples was calculated from the photos taken prior to desorption.

3 Results

Fig. 2 shows the total D desorption flux from the samples exposed to D plasma at 370 K. The shaded areas correspond to the difference between the D desorption fluxes obtained by the two RGAs used, whereas the solid lines represent their average. Four separate desorption peaks can be recognized in these TDS spectra. The first peak, found at around 450 K, is the strongest in all three cases and its intensity increases with the damage level. The other three higher-temperature peaks are found at around 670 K, 850 K, and 1050 K. They are much broader compared to the first peak and their intensity decreases with the damage level.

For all three samples shown in Fig. 2, the contribution of the *HD* signal accounts for about 43% of the total D desorption. There is a noticeable difference between *HD* and D_2 signal regarding the shape of the spectra. In all three cases, the first two peaks show stronger desorption in the D_2 signal, whereas for the third and the fourth peak *HD* signal dominates. For the first and the second peak, the *HD* signal is about 25% and $18 - 27$% of the total D desorption, respectively, whereas the D_2 signal is around $17 - 21$% of the total D desorption for the third peak and $1 - 14$% of the total D desorption for the fourth peak.

The undamaged sample and those damaged up to 0.1 dpa and 1 dpa and exposed to D plasma at 573 K, were desorbed in a different chamber using a different RGA, except for the

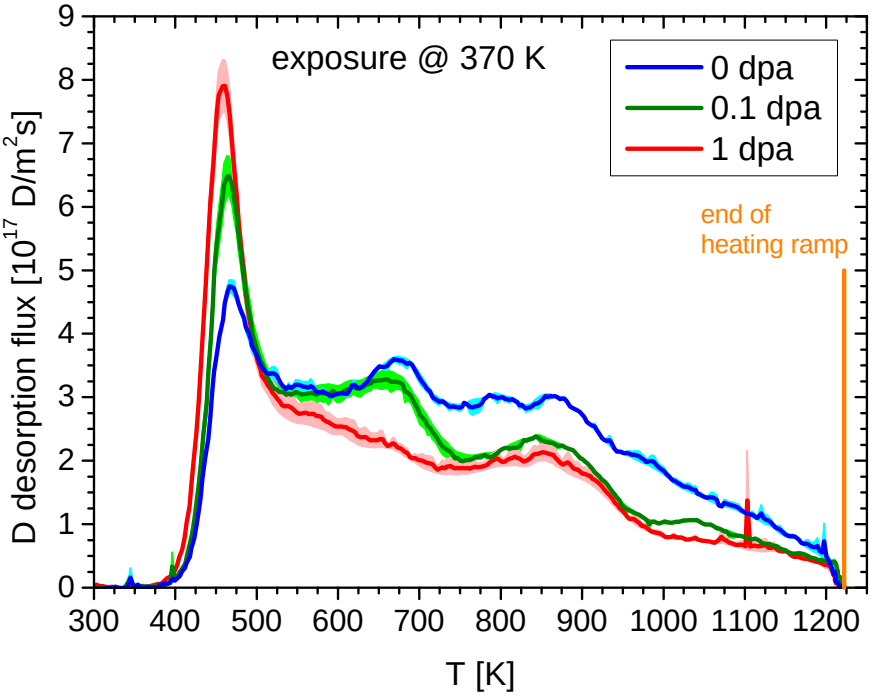

Figure 2: The total D desorption of the samples exposed to D plasma at 370 K. Heating rate was 0.3 K/s.

one damaged at 0.01 dpa. Only D_2 desorption was followed in this case, which might have an effect on the shape of the TDS spectra since the contribution of *HD* desorption was not included. The TDS spectra are shown in Fig. 3. Due to the high exposure temperature, the first peak is now absent from the spectra. The second peak is also affected by the higher exposure temperature and the start of the desorption is shifted accordingly. The third peak is strongly enhanced compared to the lower exposure temperature case, about an order of magnitude, and is the dominant peak in all three samples. The increased intensity of the peak is probably due to the faster heating rate, being 1 K/s compared to 0.3 K/s in the case of the samples in Fig. 2. The highest temperature peak (at around 1050 K) is not clearly distinguishable, possibly because of the strong high-temperature tail of the previous peak.

The sample damaged up to 0.01 dpa and exposed at 573 K (not shown) was desorbed using the same experimental setup and heating rate (0.3 K/s) as the samples exposed at 370 K, therefore, direct comparison of the spectra with the other samples exposed to 573 K is not possible. Both D_2 and *HD* signals were recorded in this case, the shape of the spectra being similar for both. The D_2 signal was weaker, being about 22% of the total D desorption for the third and dominant peak. The fourth peak is completely absent from the D_2 signal.

Obtaining an accurate D depth profile in Be using the NRA technique with ^3He ion beam is challenging due to the large penetration depth of the probing ions in Be and the low depth resolution in this case ($\sim$ 300 nm for the lowest energy and $\sim$ 1.5 μm for the

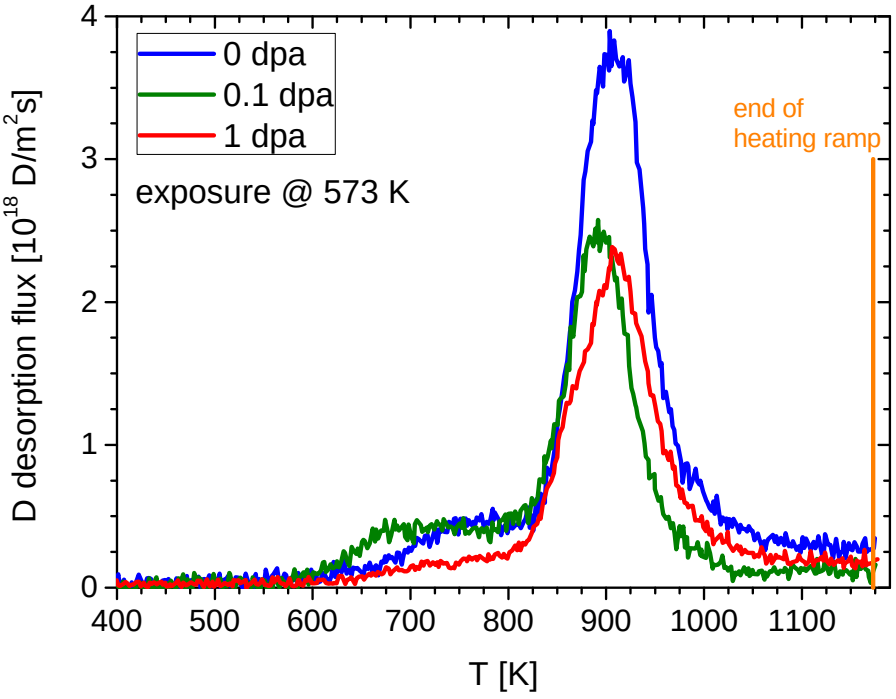

Figure 3: The D_2 desorption flux of the samples exposed to D plasma at 573 K. Heating rate was 1 K/s.

highest). However, the total D amount in the samples can be determined relatively accurately, especially using a set of multiple ion beam energies. In our case, the used ^3He energies were 500 keV, 800 keV, and 2000 keV. Fig. 4 shows the total D amounts in all the studied samples. Besides the values obtained by NRA, the total amounts calculated by integrating the TDS spectra are also included in the plot. The damaging up to 0.1 dpa has been shown to reduce the total amount of retained D by about 18% compared to the undamaged sample (comparing the NRA data). Further damaging, up to 1 dpa, seems to saturate the effect and the total amount of retained D does not change substantially. In contrast to W which already exhibits increased retention at 0.005 dpa [18], damaging the Be samples up to only 0.01 dpa does not have any perceivable effect on the amount of retained D.

In the case of plasma exposure at 370 K, the NRA and TDS data agree well and are within the uncertainties in the case of the damaged samples, even though the TDS data is consistently lower compared to NRA. Larger deviation is observed in the case of the undamaged sample, where the total D amount calculated from the TDS spectra is 11% lower compared to the total amount determined by NRA. In the case of the exposure at 573 K, please note that only D_2 desorption was followed during the TDS and the values are therefore not quantitatively comparable. Still, the trend of the data agrees with the values obtained by NRA.

TEM microscopy shows the appearance of cones on the surface of the samples exposed

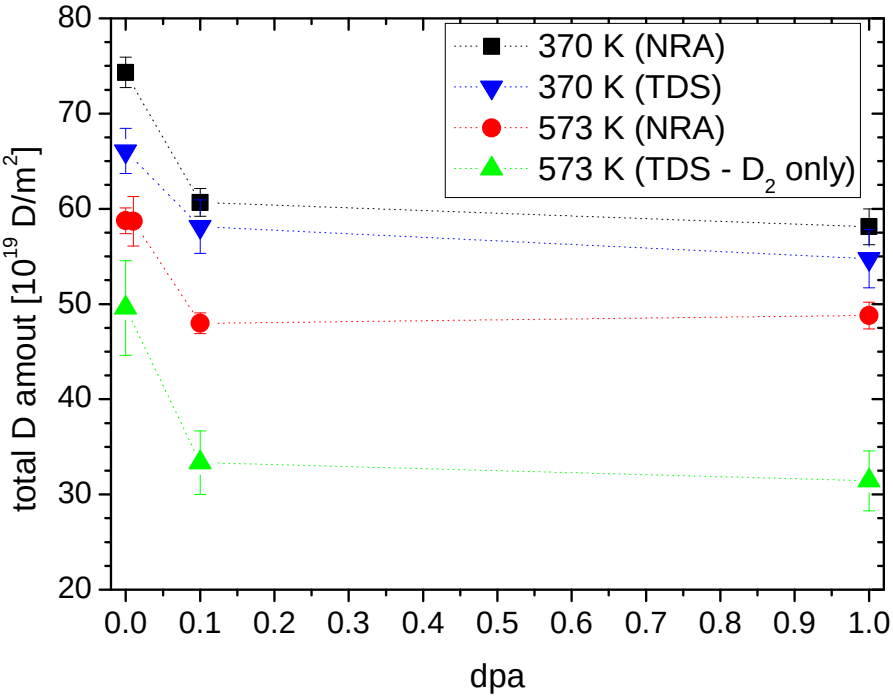

Figure 4: Total amounts of retained D, measured by NRA and TDS techniques. Note that in the case of exposure at 573 K, only D_2 signal was measured by TDS technique (green), therefore the values do not represent the total D amounts and are not directly comparable.

to D plasma at 573 K. The existence of bubbles was confirmed in all three samples studied with TEM, as seen in Fig. 5. All the samples show a large concentration of bubbles in the bulk below the cones.

Fig. 6 shows the distributions of bubble diameters for samples exposed to D plasma at 573 K. A relative increase of small bubbles (diameter < 5 nm) can be observed in the case of damaged samples compared to the undamaged one. Mean bubble diameters were determined to be 6.7 nm, 5.8 nm, and 8.1 nm for the undamaged sample and samples damaged up to 0.1 dpa and 1 dpa, respectively. Bubble densities show an increase in the case of damaged samples, being (1.3×10^{23}) m^{-3} for the undamaged sample and (1.7×10^{23}) m^{-3} and (1.8×10^{23}) m^{-3} for the 0.1 dpa and 1 dpa samples, respectively. In order to calculate the swelling, the total volume of analyzed bubbles (assuming perfect spheroids) was divided by the analyzed volume. The obtained values for calculated swelling were 2%, 8%, and 3% for 0 dpa, 0.1 dpa, and 1 dpa sample, respectively. One should note that these reported values should be taken with caution since such analysis of the TEM images could be prone to high uncertainties.

Fig. 7 shows the TEM micrographs of the cones in the case of the sample damaged up to 0.1 dpa and exposed to D plasma at 573 K. The under- and overfocused micrographs confirm the existence of small nano-bubbles (diameter < 5 nm) in the cones, which are absent in the

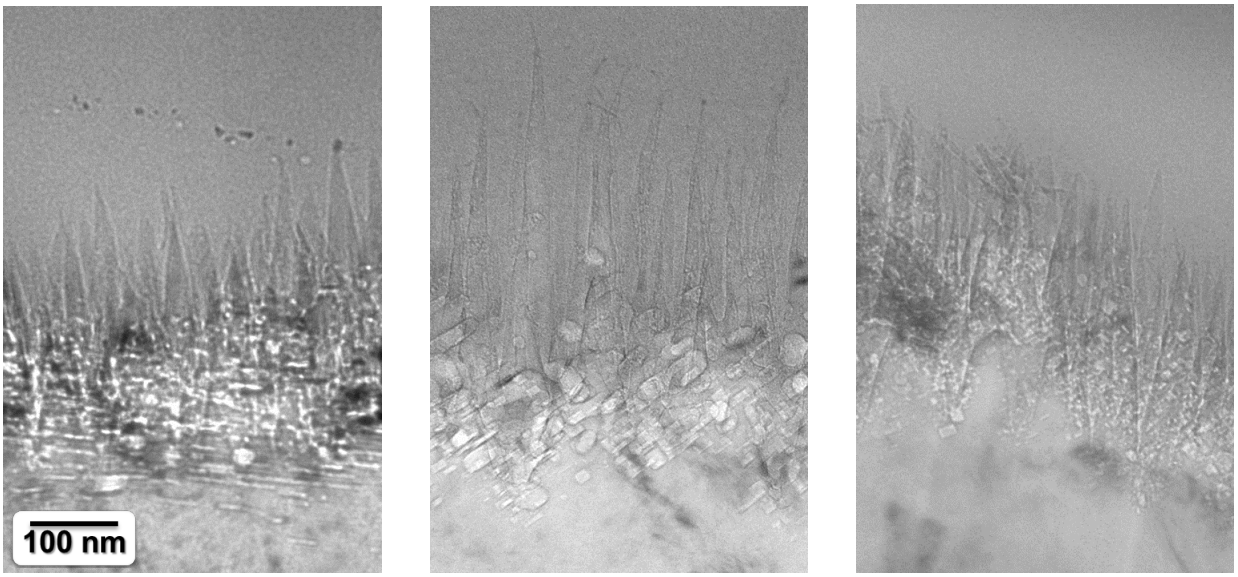

(a) 0 dpa (b) 0.1 dpa (c) 1 dpa

Figure 5: TEM micrographs of the samples, exposed to D plasma at 573 K.

case of the undamaged sample. In the sample damaged up to 1 dpa, such small-diameter bubbles also exist in the cones.

4 Discussion

The first desorption peak at around 450 K (Fig. 2) has been observed frequently in Be-D co-deposits and D ion implanted Be samples prepared under certain conditions (such as low temperature and high pressure or ion fluence), e.g. [19–21]. It has been shown that deuterium desorption from the corresponding trap does not follow the physics of the detrapping from a regular trap [22, 23] which is usually described by a simple Arrhenius term in a rate equation model, e.g. [24–26]. The current data supports previous observations of the different behavior of the first desorption peak compared to all the other peaks, since the amount of retained D increases with a higher dpa level in contrast to the decreasing trend of the other three traps. Previously studied desorption behavior [22] and modeling [23] seem to indicate the release of deuterium corresponding to this sharp desorption peak is due to the decomposition of beryllium deuteride. Whenever the concentration of solute deuterium in the material reaches the solubility limit, the precipitates of deuteride will start to form and grow if more deuterium is introduced to the material. If the first peak indeed corresponds to the decomposition of beryllium deuteride, its behavior can be explained by point defects acting as nucleation points for the formation of deuteride precipitates, which would explain the increase of their concentration with higher damage levels.

As mentioned above, the higher temperature peaks decrease for the damaged samples. The first peak (at around 670 K) is not strongly affected when the samples are damaged up to only 0.1 dpa, but decreases noticeably for 1 dpa. The other two peaks (at around 850

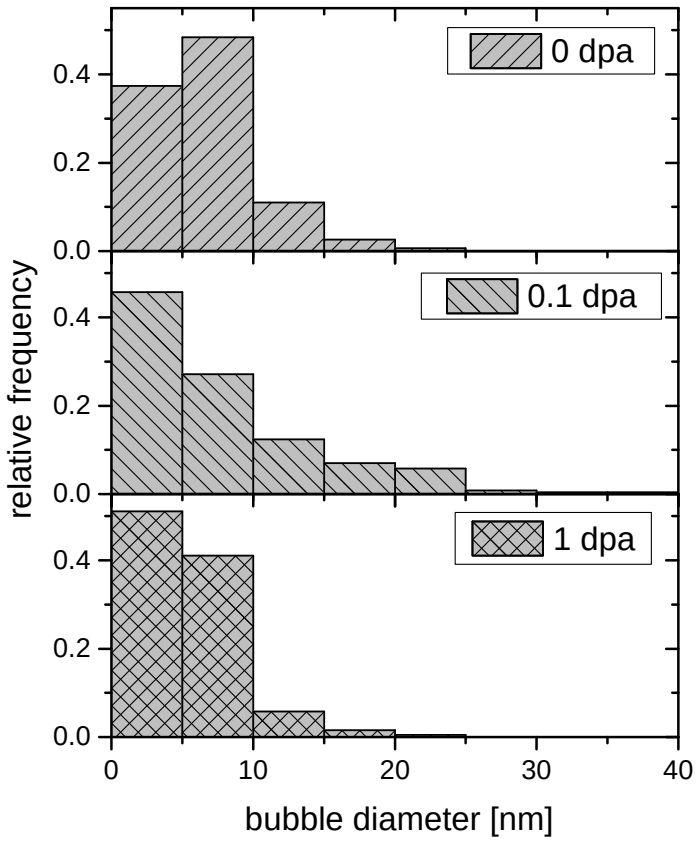

Figure 6: Distributions of bubble diameters for undamaged sample and samples damaged up to 0.1 dpa and 1 dpa, exposed to D plasma at 573 K.

K and 1050 K) show a different behavior, namely their intensity drops already for 0.1 dpa, but for stronger damaging the effect seems to saturate and only a small decrease is observed. The exact same behavior is observed in both sets of samples, exposed at 370 K and 573 K (Fig. 2 and Fig. 3, respectively). Note the small offset in the case of the sample damaged up to 0.1 dpa and exposed at 573 K, which is probably due to experimental uncertainties.

Ion-damaging is known to reduce the thermal conductivity of the material [1, 2]. Since the temperature of the sample is measured by a thermocouple at the back of the sample during the plasma exposure, the reduced thermal conductivity would lead to the actual surface temperature being considerably higher. One could then argue that this could in effect reduce the amount of retained deuterium in the damaged samples, as is observed in our experiments. However, such a claim can be easily disproved by studying the shape of the TDS spectra. If the surface temperature was indeed considerably higher, the TDS spectra would reflect that and the damaged samples exposed at low temperature would show the spectra similar to the samples exposed at higher temperature, especially regarding the onset temperature of D

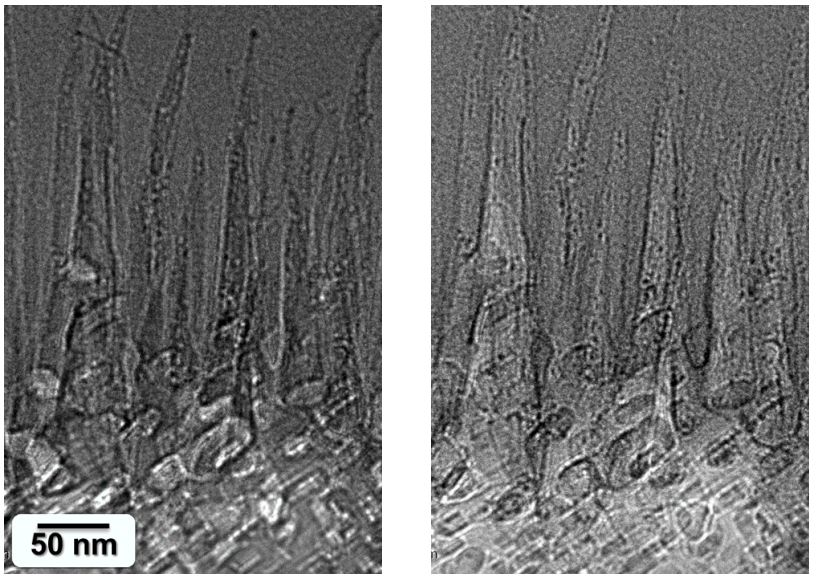

(a) underfocus (b) overfocus

Figure 7: Over- and underfocused TEM micrographs of the sample damaged up to 0.1 dpa and exposed to D plasma at 573 K.

desorption. Since we do not see such a change and the spectra of the samples exposed at low temperature all show the exact same peaks, we can conclude that the surface temperature must have been very similar for damaged and undamaged samples. Moreover, estimating the surface temperature by solving a 1-D heat equation confirms that reducing the thermal conductivity in the first 2 μm by two orders of magnitude results in a change of surface temperature by less than 1 K.

The fact that the undamaged sample shows the same peaks in the TDS spectrum as the damaged ones and, moreover, has the highest amount of trapped deuterium indicates that low-energy D plasma is able to create substantial damage to the Be crystal lattice. This could be explained by the relatively low displacement energy of Be ($\sim 20 - 21$ eV) [27, 28] as well as its low mass which means that energy is efficiently transferred to the Be atom during the binary head-on collision. The maximum energy transfer for 40 eV D ions is in fact larger than the displacement energy for Be, being 23.8 eV. Since the plasma-exposed undamaged sample shows the largest concentration of traps, plasma exposure itself has to be the dominant defect creation mechanism. This can be justified by high plasma-exposure fluence. Even though the energy of the incoming D ions is much lower compared to the energy of the O ion beam and therefore only a small number of Frenkel pairs can be created per D ion, the total ion fluence for plasma exposure is orders of magnitude higher. Moreover, the ion range in plasma exposure is limited only to very close to the surface, where in the case of the energetic O ion beam less energy is transferred to the material and therefore the amount of damage done is lower (see Fig. 1). Deuterium retention in Be has been shown to saturate with increasing fluence [19, 29, 30], which indicates a lack of diffusion into the bulk, therefore it cannot be affected by the defects created by the O ion beam deeper in the bulk. Moreover, previous studies on W showed substantial plasma-induced displacement

defect creation even in low-energy D plasma, extending up to $\sim$ 10 nm under the surface and causing a super-saturated deuterium layer with D/W as high as 0.1 [31]. This can be explained by significantly reduced displacement energy in the presence of D in the crystal lattice. If similar effect also takes place in Be, this would further enhance the plasma-induced damage which we seem to observe in our data.

The observed decrease of D retention in the damaged samples could be explained by ion-damage assisted growth of large networks of interconnected bubbles. The saturation of D retention in Be which can be explained by the growth of bubbles, which eventually interconnect and open towards the surface, strongly increasing the porosity of the surface [30, 32–34]. Therefore, the recycling of deuterium increases and saturates its retention by reaching the steady state of implantation and recombination. As can be seen on the TEM micrographs (Figs. 5 and 7), the small nano-bubbles only exist in the cones of the pre-damaged samples. The small size of these bubbles can be explained by lower D concentration in those areas, since most of the D ions end up close to the end of the implantation range, where D concentration is the highest and where, consequently, a large number of bigger bubbles is observed. However, since the nano-bubbles in the cones exist only in the case of the damaged samples, one can conclude that ion-induced defects assist in bubble growth. The growth of extensive bubble networks is thus expedited in the damaged samples and the equilibrium between implantation and recombination is reached sooner, leaving a lower amount of deuterium retained in the material.

5 Conclusion

The effect of ion-damaging on deuterium retention in beryllium has been studied using NRA, TDS, and TEM techniques. Retention in the samples damaged up to 0.1 dpa was shown to be about 18% lower compared to the undamaged samples, whereas further damaging up to 1 dpa seems to saturate the effect and does not substantially change the retention. Damaging up to only 0.01 dpa does not have any effect on D retention within the uncertainties.

The TDS spectra of the samples exposed to D plasma at 370 K show four desorption peaks. The lowest-temperature peak behaves differently than the others and increases in intensity when increasing the damage level. The other three peaks decrease with the damage level. The fact that the undamaged sample shows the same shape of the TDS spectrum and retains the highest amount of deuterium indicates that plasma exposure is the dominant damaging mechanism. The reduction of retained deuterium in damaged samples can be explained by pre-existing defects expediting bubble growth during plasma exposure, leading to a surface with high open-porosity.

In contrast to W, where damaging is known to strongly increase hydrogen isotope retention, Be shows a relatively weak influence of pre-existing defects on D retention after plasma exposure. Ignoring other detrimental effects of damaging on the material, these results indicate there could be little concern regarding the increase of fuel retention in displacement-damaged Be for ITER. However, caution should be taken when extrapolating results obtained by ion irradiation to neutron irradiation, since it is a well known fact that there exist a few important differences between the two. For example, in the case of neutrons, nuclear reactions will lead to transmutations and gas production in the material, while no such concerns exist

for ion irradiation. Therefore, further studies are needed to draw more definite conclusions on the implication of neutron irradiation on fuel retention in ITER first wall.

ACKNOWLEDGMENT

This work has been carried out within the framework of the EUROfusion Consortium and has received funding from the Euratom research and training programme 2014-2018 and 2019-2020 under grant agreement No 633053. This work was done within the EUROfusion work project PFC. The views and opinions expressed herein do not necessarily reflect those of the European Commission. This work was also supported by the U.S. Department of Energy grant #DE-FG02-07ER54912 as part of the US-EU Bilateral Collaboration on Mixed Materials for ITER.

References

[1] F. Hofmann, D. Mason, J. Eliason, A. Maznev, K. Nelson, and S. Dudarev, "Non-Contact Measurement of Thermal Diffusivity in Ion-Implanted Nuclear Materials," *Sci. Rep.*, vol. 5, p. 16042, 2015.

[2] G. Tynan, R. Doerner, J. Barton, R. Chen, S. cui, M. Simmonds, Y. Wang, J. Weaver, N. Mara, and S. Pathak, "Deuterium retention and thermal conductivity in ion-beam displacement-damaged tungsten," *Nucl. Mater. Energy*, vol. 12, p. 164, 2017.

[3] J. Roth, E. Tsitrone, A. Loarte, Th. Loarer, G. Counsell, R. Neu, V. Philipps, S. Brezinsek, M. Lehnen, P. Coad, Ch. Grisolia, K. Schmid, K. Krieger, A. Kallenbach, B. Lipschultz, R. Doerner, R. Causey, V. Alimov, W. Shu, O. Ogorodnikova, A. Kirschner, G. Federici, A. Kukushkin, EFDA PWI Task Force, ITER PWI Team, Fusion for Energy, and ITPA SOL/DIV, "Recent analysis of key plasma wall interactions issues for ITER," *J. Nucl. Mater.*, vol. 390-391, p. 1, 2009.

[4] M. Fukumoto, H. Kashiwagi, Y. Ohtsuka, Y. Ueda, M. Taniguchi, T. Inoue, K. Sakamoto, J. Yagyu, T. Arai, I. Takagi, and T. Kawamura, "Deuterium trapping in tungsten damaged by high-energy hydrogen ion irradiation," *J. Nucl. Mater.*, vol. 390-391, p. 572, 2009.

[5] W. Wampler and R. Doerner, "The influence of displacement damage on deuterium retention in tungsten exposed to plasma," *Nucl. Fusion*, vol. 49, p. 115023, 2009.

[6] V. Chakin, V. Kazakov, A. Teykovtsev, V. Pimenov, G. Shiimansky, Z. Ostrovsky, D. Suslov, R. Latypov, S. Belozerov, and I. Kupriyanov, "High dose neutron irradiation damage in beryllium as blanket material," *Fusion Eng. Des.*, vol. 58-59, p. 535, 2001.

[7] V. Chakin, A. Posevin, and R. Latypov, "Radiation damage in beryllium at $70-440$°C and neutron fluence $(0.3-18)\cdot 10^{22}$ cm^{-2}($E_n > 0.1$ MeV)," *At. Energy*, vol. 101, p. 743, 2006.

[8] M. Gilbert, S.L.Dudarev, S. Zheng, L. Packer, and J.-Ch. Sublet, "An integrated model for materials in a fusion power plant: transmutation, gas production, and helium embrittlement under neutron irradiation," *Nucl. Fusion*, vol. 52, p. 083019, 2012.

[9] ASTM International, West Conshohocken, PA, *ASTM E521-16, Standard Practice for Investigating the Effects of Neutron Radiation Damage Using Charged-Particle Irradiation*, 2016.

[10] M. Mayer, S. Möller, M. Rubel, A. Widdowson, S. Charisopoulos, T. Ahlgren, E. Alves, G. Apostolopoulos, N. Barradas, and S. Donnelly, "Ion beam analysis of fusion plasma-facing materials and components: facilities and research challenges," *Nucl. Fusion*, vol. 60, p. 025001, 2020.

[11] www.srim.org.

[12] R. Doerner, M. Baldwin, and K. Schmid, "The Influence of a Beryllium Containing Plasma on the Evolution of a Mixed-Material Surface," *Phys. Scr.*, vol. T111, p. 75, 2004.

[13] K. Schmid and U. von Toussaint, "Statistically sound evaluation of trace element depth profiles by ion beam analysis," *Nuclear Instrum. Methods Phys. Res. B*, vol. 281, p. 64, 2012.

[14] M. Baldwin, T. Schwarz-Selinger, and R. Doerner, "Experimental study and modelling of deuterium thermal release from Be-D co-deposited layers," *Nucl. Fusion*, vol. 54, p. 073005, 2014.

[15] J. Yu, M. Simmonds, M.J.Baldwin, and R. Doerner, "Deuterium desorption from tungsten using laser heating," *Nucl. Mater. Energy*, vol. 12, p. 749, 2017.

[16] M. Simmonds, Y. Wang, J. Barton, M.J.Baldwin, J. Yu, R. Doerner, and G. Tynan, "Reduced deuterium retention in simultaneously damaged and annealed tungsten," *J. Nucl. Mater.*, vol. 494, p. 67, 2017.

[17] M. Miyamoto, T. Watanabe, H. Nagashima, D. Nishijima, R. Doerner, S. Krasheninnikov, A. Sagara, and N. Yoshida, "In situ transmission electron microscope observation of the formation of fuzzy structures on tungsten," *Phys. Scr.*, vol. T159, p. 014028, 2014.

[18] O. Ogorodnikova and V. Gann, "Simulation of neutron-induced damage in tungsten by irradiation with energetic self-ions," *J. Nucl. Mater.*, vol. 460, p. 60, 2015.

[19] M. Reinelt, A. Allouche, M. Oberkofler, and Ch. Linsmeier, "Retention mechanisms and binding states of deuterium implanted into beryllium," *New J. Phys.*, vol. 11, p. 043023, 2009.

[20] M. Baldwin, T. Schwarz-Selinger, and R. Doerner, "D retention in Be exposed to fusion relevant mixed species $D_2 - He$ plasma," *Nucl. Mater. Energy*, vol. 12, p. 678, 2017.

[21] A. Založnik, M. Baldwin, R. Doerner, T. Schwarz-Selinger, and S. Brezinsek, "The influence of helium on deuterium retention in beryllium co-deposits," *J. Nucl. Mater.*, vol. 512, p. 25, 2018.

[22] M. Baldwin, M. Simmonds, G. De Temmerman, and R. Doerner, "Deuterium retention in Be-D co-deposits formed over an ITER relevant parameter space," *Phys. Scr.*, vol. T171, p. 014014, 2020.

[23] A. Založnik, M. Baldwin, , M. Simmonds, and R. Doerner, "Modeling the sharp deuterium release from beryllium co-deposits," *Nucl. Fusion*, vol. 59, p. 126027, 2019.

[24] G. Longhurst, *TMAP7 User Manual INEEL/EXT-04–02352, Rev. 2.* Idaho National Engineering & Environment Laboratory, Idaho Falls, ID, 2008.

[25] K. Schmid, V. Rieger, and A. Manhard, "Comparison of hydrogen retention in W and W/Ta alloys," *J. Nucl. Mater.*, vol. 426, p. 247, 2012.

[26] O. Ogorodnikova, J. Roth, and M. Mayer, "Deuterium retention in tungsten in dependence of the surface conditions," *J. Nucl. Mater.*, vol. 313-316, p. 469, 2003.

[27] V. Borodin and P. Vladimirov, "Damage production in atomic displacement cascades in beryllium," *Nucl. Mater. Energy*, vol. 9, p. 216, 2016.

[28] P. Vladimirov and V. Borodin, "First-principles and classical molecular dynamics study of threshold displacement energy in beryllium," *Nuclear Instrum. Mathods Phys. Res. B*, vol. 393, p. 195, 2017.

[29] W. Wampler, "Retention and thermal release of deuterium implanted in berylliun," *J. Nucl. Mater.*, vol. 122-123, p. 1598, 1984.

[30] R. Doerner, A. Grossman, S. Luckhardt, R. Seraydarian, F. Sze, D. Whyte, and R. Conn, "Response of beryllium to deuterium plasma bombardment," *J. Nucl. Mater.*, vol. 257, p. 51, 1998.

[31] L. Gao, W. Jacob, U. von Toussaint, A. Manhard, M. Balden, K. Schmid, and T. Schwarz-Selinger, "Deuterium supersaturation in low-energy plasma-loaded tungsten surfaces," *Nucl. Fusion*, vol. 57, p. 016026, 2017.

[32] V. Chernikov, V.Kh. Alimov, A. Markin, A. Gorodetsky, S. Kanashenko, A. Zakharov, and I. Kupriyanov, "Gas-induced swelling of beryllium implanted with deuterium ions," *J. Nucl. Mater.*, vol. 233-237, p. 860, 1996.

[33] A. Markin, V. Chernikov, S.Yu. Rybakov, and A. Zakharov, "Thermal desorption of deuterium implanted into beryllium," *J. Nucl. Mater.*, vol. 233-237, p. 865, 1996.

[34] V.Kh. Alimov, V. Chernikov, and A. Zakharov, "Depth distribution of deuterium atoms and molecules in beryllium implanted with D ions," *J. Nucl. Mater.*, vol. 241-243, p. 1047, 1997.